Measurement of the W mass in e^+e^- collisions at production threshold

R. Barate, D. Buskulic, D. Decamp, P. Ghez, C. Goy, J P. Lees, A. Lucotte, M N. Minard, J Y. Nief, B. Pietrzyk, et al.

EUROPEAN LABORATORY FOR PARTICLE PHYSICS (CERN)

CERN-PPE/97-025
4 March 1997

Measurement of the W Mass in $\mathrm{e^+e^-}$ Collisions at Production Threshold

The ALEPH Collaboration[1)]

Abstract

In June 1996, the LEP centre-of-mass energy was raised to 161 GeV. Pair production of W bosons in $\mathrm{e^+e^-}$ collisions was observed for the first time by the LEP experiments. An integrated luminosity of 11 pb^{-1} was recorded in the ALEPH detector, in which WW candidate events were observed. In 6 events both Ws decay leptonically. In 16 events, one W decays leptonically, the other into hadrons. In the channel where both Ws decay into hadrons, a signal was separated from the large background by means of several multi-variate analyses. The W pair cross-section is measured to be

$$\sigma_{\mathrm{WW}} = 4.23 \pm 0.73(\mathrm{stat.}) \pm 0.19(\mathrm{syst.}) \ \mathrm{pb}.$$

From this cross-section, the W mass is derived within the framework of the Standard Model:

$$m_{\mathrm{W}} = 80.14 \pm 0.34(\mathrm{stat.}) \pm 0.09(\mathrm{syst.}) \pm 0.03(\mathrm{LEP\ energy})\ \mathrm{GeV}/c^2.$$

(Submitted to Phys. Lett. B)

[1)] see next pages for the list of authors

The ALEPH Collaboration

R. Barate, D. Buskulic, D. Decamp, P. Ghez, C. Goy, J.-P. Lees, A. Lucotte, M.-N. Minard, J.-Y. Nief, B. Pietrzyk

Laboratoire de Physique des Particules (LAPP), IN^{2}P^3-CNRS, 74019 Annecy-le-Vieux Cedex, France

M.P. Casado, M. Chmeissani, P. Comas, J.M. Crespo, M. Delfino, E. Fernandez, M. Fernandez-Bosman, Ll. Garrido,[15] A. Juste, M. Martinez, R. Miquel, Ll.M. Mir, S. Orteu, C. Padilla, I.C. Park, A. Pascual, J.A. Perlas, I. Riu, F. Sanchez, F. Teubert

Institut de Fisica d'Altes Energies, Universitat Autonoma de Barcelona, 08193 Bellaterra (Barcelona), Spain[7]

A. Colaleo, D. Creanza, M. de Palma, G. Gelao, G. Iaselli, G. Maggi, M. Maggi, N. Marinelli, S. Nuzzo, A. Ranieri, G. Raso, F. Ruggieri, G. Selvaggi, L. Silvestris, P. Tempesta, A. Tricomi,[3] G. Zito

Dipartimento di Fisica, INFN Sezione di Bari, 70126 Bari, Italy

X. Huang, J. Lin, Q. Ouyang, T. Wang, Y. Xie, R. Xu, S. Xue, J. Zhang, L. Zhang, W. Zhao

Institute of High-Energy Physics, Academia Sinica, Beijing, The People's Republic of China[8]

D. Abbaneo, R. Alemany, A.O. Bazarko,[1] U. Becker, P. Bright-Thomas, M. Cattaneo, F. Cerutti, H. Drevermann, R.W. Forty, M. Frank, R. Hagelberg, J. Harvey, P. Janot, B. Jost, E. Kneringer, J. Knobloch, I. Lehraus, G. Lutters, P. Mato, A. Minten, L. Moneta, A. Pacheco, J.-F. Pusztaszeri, F. Ranjard, P. Rensing,[2] G. Rizzo, L. Rolandi, D. Schlatter, M. Schmitt, O. Schneider, W. Tejessy, I.R. Tomalin, H. Wachsmuth, A. Wagner

European Laboratory for Particle Physics (CERN), 1211 Geneva 23, Switzerland

Z. Ajaltouni, A. Barrès, C. Boyer, A. Falvard, C. Ferdi, P. Gay, C . Guicheney, P. Henrard, J. Jousset, B. Michel, S. Monteil, J-C. Montret, D. Pallin, P. Perret, F. Podlyski, J. Proriol, P. Rosnet, J.-M. Rossignol

Laboratoire de Physique Corpusculaire, Université Blaise Pascal, IN^{2}P^3-CNRS, Clermont-Ferrand, 63177 Aubière, France

T. Fearnley, J.B. Hansen, J.D. Hansen, J.R. Hansen, P.H. Hansen, B.S. Nilsson, B. Rensch, A. Wäänänen

Niels Bohr Institute, 2100 Copenhagen, Denmark[9]

G. Daskalakis, A. Kyriakis, C. Markou, E. Simopoulou, A. Vayaki

Nuclear Research Center Demokritos (NRCD), Athens, Greece

A. Blondel, J.C. Brient, F. Machefert, A. Rougé, M. Rumpf, A. Valassi,[6] H. Videau

Laboratoire de Physique Nucléaire et des Hautes Energies, Ecole Polytechnique, IN^{2}P^3-CNRS, 91128 Palaiseau Cedex, France

E. Focardi, G. Parrini, K. Zachariadou

Dipartimento di Fisica, Università di Firenze, INFN Sezione di Firenze, 50125 Firenze, Italy

M. Corden, C. Georgiopoulos, D.E. Jaffe

Supercomputer Computations Research Institute, Florida State University, Tallahassee, FL 32306-4052, USA [13,14]

A. Antonelli, G. Bencivenni, G. Bologna,[4] F. Bossi, P. Campana, G. Capon, D. Casper, V. Chiarella, G. Felici, P. Laurelli, G. Mannocchi,[5] F. Murtas, G.P. Murtas, L. Passalacqua, M. Pepe-Altarelli

Laboratori Nazionali dell'INFN (LNF-INFN), 00044 Frascati, Italy

L. Curtis, S.J. Dorris, A.W. Halley, I.G. Knowles, J.G. Lynch, V. O'Shea, C. Raine, J.M. Scarr, K. Smith, P. Teixeira-Dias, A.S. Thompson, E. Thomson, F. Thomson, R.M. Turnbull

Department of Physics and Astronomy, University of Glasgow, Glasgow G12 8QQ,United Kingdom[10]

C. Geweniger, G. Graefe, P. Hanke, G. Hansper, V. Hepp, E.E. Kluge, A. Putzer, M. Schmidt, J. Sommer, K. Tittel, S. Werner, M. Wunsch

Institut für Hochenergiephysik, Universität Heidelberg, 69120 Heidelberg, Fed. Rep. of Germany[16]

R. Beuselinck, D.M. Binnie, W. Cameron, P.J. Dornan, M. Girone, S. Goodsir, E.B. Martin, P. Morawitz, A. Moutoussi, J. Nash, J.K. Sedgbeer, A.M. Stacey, M.D. Williams

Department of Physics, Imperial College, London SW7 2BZ, United Kingdom[10]

G. Dissertori, V.M. Ghete, P. Girtler, D. Kuhn, G. Rudolph

Institut für Experimentalphysik, Universität Innsbruck, 6020 Innsbruck, Austria[18]

A.P. Betteridge, C.K. Bowdery, P. Colrain, G. Crawford, A.J. Finch, F. Foster, G. Hughes, R.W. Jones, T. Sloan, E.P. Whelan, M.I. Williams

Department of Physics, University of Lancaster, Lancaster LA1 4YB, United Kingdom[10]

C. Hoffmann, K. Jakobs, K. Kleinknecht, G. Quast, B. Renk, E. Rohne, H.-G. Sander, P. van Gemmeren, C. Zeitnitz

Institut für Physik, Universität Mainz, 55099 Mainz, Fed. Rep. of Germany[16]

J.J. Aubert, C. Benchouk, A. Bonissent, G. Bujosa, D. Calvet, J. Carr, P. Coyle, C. Diaconu, N. Konstantinidis, O. Leroy, F. Motsch, P. Payre, D. Rousseau, M. Talby, A. Sadouki, M. Thulasidas, A. Tilquin, K. Trabelsi

Centre de Physique des Particules, Faculté des Sciences de Luminy, IN^2*P*^{3}*-CNRS, 13288 Marseille, France*

M. Aleppo, F. Ragusa[21]

Dipartimento di Fisica, Università di Milano e INFN Sezione di Milano, 20133 Milano, Italy.

R. Berlich, W. Blum, V. Büscher, H. Dietl, F. Dydak,[21] G. Ganis, C. Gotzhein, H. Kroha, G. Lütjens, G. Lutz, W. Männer, H.-G. Moser, R. Richter, A. Rosado-Schlosser, S. Schael, R. Settles, H. Seywerd, R. St. Denis, H. Stenzel, W. Wiedenmann, G. Wolf

Max-Planck-Institut für Physik, Werner-Heisenberg-Institut, 80805 München, Fed. Rep. of Germany[16)]

J. Boucrot, O. Callot,[21] S. Chen, A. Cordier, M. Davier, L. Duflot, J.-F. Grivaz, Ph. Heusse, A. Höcker, A. Jacholkowska, M. Jacquet, D.W. Kim,[22] F. Le Diberder, J. Lefrançois, A.-M. Lutz, I. Nikolic, M.-H. Schune, S. Simion, E. Tournefier, J.-J. Veillet, I. Videau, D. Zerwas

Laboratoire de l'Accélérateur Linéaire, Université de Paris-Sud, IN^2*P*^{3}*-CNRS, 91405 Orsay Cedex, France*

P. Azzurri, G. Bagliesi, G. Batignani, S. Bettarini, C. Bozzi, G. Calderini, M. Carpinelli, M.A. Ciocci, V. Ciulli, R. Dell'Orso, R. Fantechi, I. Ferrante, A. Giassi, A. Gregorio, F. Ligabue, A. Lusiani, P.S. Marrocchesi, A. Messineo, F. Palla, G. Sanguinetti, A. Sciabà, P. Spagnolo, J. Steinberger, R. Tenchini, G. Tonelli,[20] C. Vannini, A. Venturi, P.G. Verdini

Dipartimento di Fisica dell'Università, INFN Sezione di Pisa, e Scuola Normale Superiore, 56010 Pisa, Italy

G.A. Blair, L.M. Bryant, J.T. Chambers, Y. Gao, M.G. Green, T. Medcalf, P. Perrodo, J.A. Strong, J.H. von Wimmersperg-Toeller

Department of Physics, Royal Holloway & Bedford New College, University of London, Surrey TW20 OEX, United Kingdom[10]

D.R. Botterill, R.W. Clifft, T.R. Edgecock, S. Haywood, P. Maley, P.R. Norton, J.C. Thompson, A.E. Wright

Particle Physics Dept., Rutherford Appleton Laboratory, Chilton, Didcot, Oxon OX11 OQX, United Kingdom[10]

B. Bloch-Devaux, P. Colas, W. Kozanecki, E. Lançon, M.C. Lemaire, E. Locci, P. Perez, J. Rander, J.-F. Renardy, A. Roussarie, J.-P. Schuller, J. Schwindling, A. Trabelsi, B. Vallage

CEA, DAPNIA/Service de Physique des Particules, CE-Saclay, 91191 Gif-sur-Yvette Cedex, France[17]

S.N. Black, J.H. Dann, H.Y. Kim, A.M. Litke, M.A. McNeil, G. Taylor

Institute for Particle Physics, University of California at Santa Cruz, Santa Cruz, CA 95064, USA[19]

C.N. Booth, R. Boswell, C.A.J. Brew, S. Cartwright, F. Combley, M.S. Kelly, M. Lehto, W.M. Newton, J. Reeve, L.F. Thompson

Department of Physics, University of Sheffield, Sheffield S3 7RH, United Kingdom[10]

K. Affholderbach, A. Böhrer, S. Brandt, G. Cowan, J. Foss, C. Grupen, P. Saraiva, L. Smolik, F. Stephan

Fachbereich Physik, Universität Siegen, 57068 Siegen, Fed. Rep. of Germany[16]

M. Apollonio, L. Bosisio, R. Della Marina, G. Giannini, B. Gobbo, G. Musolino

Dipartimento di Fisica, Università di Trieste e INFN Sezione di Trieste, 34127 Trieste, Italy

J. Putz, J. Rothberg, S. Wasserbaech, R.W. Williams

Experimental Elementary Particle Physics, University of Washington, WA 98195 Seattle, U.S.A.

S.R. Armstrong, E. Charles, P. Elmer, D.P.S. Ferguson, Y.S. Gao,[12] S. González, T.C. Greening, O.J. Hayes, H. Hu, S. Jin, P.A. McNamara III, J.M. Nachtman, J. Nielsen, W. Orejudos, Y.B. Pan, Y. Saadi, I.J. Scott, J. Walsh, Sau Lan Wu, X. Wu, J.M. Yamartino, G. Zobernig

Department of Physics, University of Wisconsin, Madison, WI 53706, USA[11]

[1)] Now at Princeton University, Princeton, NJ 08544, U.S.A.
[2)] Now at Dragon Systems, Newton, MA 02160, U.S.A.
[3)] Also at Dipartimento di Fisica, INFN Sezione di Catania, Catania, Italy.
[4)] Also Istituto di Fisica Generale, Università di Torino, Torino, Italy.
[5)] Also Istituto di Cosmo-Geofisica del C.N.R., Torino, Italy.
[6)] Supported by the Commission of the European Communities, contract ERBCHBICT941234.
[7)] Supported by CICYT, Spain.
[8)] Supported by the National Science Foundation of China.
[9)] Supported by the Danish Natural Science Research Council.
[10)] Supported by the UK Particle Physics and Astronomy Research Council.
[11)] Supported by the US Department of Energy, grant DE-FG0295-ER40896.
[12)] Now at Harvard University, Cambridge, MA 02138, U.S.A.
[13)] Supported by the US Department of Energy, contract DE-FG05-92ER40742.
[14)] Supported by the US Department of Energy, contract DE-FC05-85ER250000.
[15)] Permanent address: Universitat de Barcelona, 08208 Barcelona, Spain.
[16)] Supported by the Bundesministerium für Bildung, Wissenschaft, Forschung und Technologie, Fed. Rep. of Germany.
[17)] Supported by the Direction des Sciences de la Matière, C.E.A.
[18)] Supported by Fonds zur Förderung der wissenschaftlichen Forschung, Austria.
[19)] Supported by the US Department of Energy, grant DE-FG03-92ER40689.
[20)] Also at Istituto di Matematica e Fisica, Università di Sassari, Sassari, Italy.
[21)] Also at CERN, 1211 Geneva 23, Switzerland.
[22)] Permanent address: Kangnung National University, Kangnung, Korea.

1 Introduction

Production of pairs of W bosons is one of the major goals of the LEP2 programme. In June 1996, the LEP centre-of-mass energy reached the W pair threshold of 161 GeV. So far, the discovery [1, 2] and studies of W bosons have taken place in $\mathrm{p\overline{p}}$ collisions, where single W production is possible. Large samples of single Ws decaying into $\mathrm{e}\nu_{\mathrm{e}}$ and $\mu\nu_{\mu}$ have been used to measure the W mass [3, 4]. The present precision of the world average [4] is 125 MeV/c^2.

At LEP2, the measurement of the W mass should improve significantly: Ws can be detected through all decay modes, and the centre-of-mass energy can be known precisely. The cross-section at a well chosen energy close to W-pair production threshold provides a sensitive measurement of the W mass, with very little dependence on the other parameters of the Standard Model [5]. The comparison of this measurement with the prediction based on the Z mass and the Fermi constant constitutes a sensitive probe of electroweak radiative corrections. Given the present precision [6] on the top quark mass, this could give indications on the mass of the as-yet undiscovered Higgs boson or reveal new physics.

This letter presents a measurement of the W pair cross-section at threshold and subsequent extraction of the W mass, using data collected between June and August 1996 with the ALEPH detector. An integrated luminosity of 11.08 ± 0.08 pb^{-1} was recorded, at a mean centre-of-mass energy of 161.314 ± 0.054 GeV [7]. This letter is organized as follows. First, the ALEPH detector and the luminosity measurement are recalled. The physical processes occurring at the considered energy, and the related Monte Carlo programs used to simulate them, are presented together with the definition of the W pair production cross-section. The selection procedures for the different decay channels are described next, followed by the cross-section and W mass results.

2 The ALEPH detector

A detailed description of the ALEPH detector can be found in Ref. [8] and of its performance in Ref. [9]. Charged particles are detected in the central part of the detector. From the beam crossing point outwards, a silicon vertex detector, a cylindrical drift chamber, and a large time projection chamber (TPC), measure up to 31 coordinates along the charged particle trajectories. A 1.5 T axial magnetic field is provided by a superconducting solenoidal coil. A $1/p_T$ resolution of 6×10^{-4} $(\mathrm{GeV}/c)^{-1}$ is achieved. Hereafter, charged particle tracks reconstructed from at least four hits in the TPC and originating from within a cylinder of 2 cm radius and 20 cm length, centred on the nominal interaction point and parallel to the beam axis, are called *good tracks*.

Electrons and photons are identified in the electromagnetic calorimeter by their characteristic longitudinal and transverse shower developments. The calorimeter, a lead wire-plane sampling device with fine read-out segmentation and total thickness of 22 radiation lengths at normal incidence, provides a relative energy resolution of $0.18/\sqrt{E}$ (E in GeV).

Muons are identified by their characteristic penetration pattern in the hadron calorimeter, a 1.2 m thick iron yoke instrumented with 23 layers of streamer tubes, together with two surrounding layers of muon chambers. In association with the electromagnetic calorimeter, the hadron calorimeter also provides a measurement of the energy of charged and neutral hadrons with a relative resolution of $0.85/\sqrt{E}$ (E in GeV).

The total visible energy and momentum, and therefore also the missing energy, are

evaluated by an energy-flow reconstruction algorithm [9] which combines all of the above measurements, supplemented at low polar angles by the energy detected in the luminosity calorimeters. The algorithm provides also a list of charged and neutral reconstructed objects, called *energy-flow particles*, from which jets are reconstructed with a typical angular resolution of 30 mrad in space. The detector contribution to the jet energy resolution is approximately parameterized as $\sigma_E = (0.60\sqrt{E} + 0.6)\mathrm{GeV} \times (1 + \cos^2\theta)$, where E (in GeV) and θ are the jet energy and polar angle, respectively.

Luminosity is measured with small-angle Bhabha events, using lead-proportional wire sampling calorimeters covering polar angles from 45 to 160 mrad on both sides of the interaction point [10]. The accepted Bhabha cross-section is approximately 5.9 nb, calculated by Monte Carlo using the BHLUMI [11] event generator. The statistical error is 0.4% and the systematic uncertainty 0.6%. The background contamination is less than 0.1%. The integrated luminosity accumulated when all essential parts of the detector were active is 11.08 ± 0.08 pb^{-1}.

3 Physics processes and definition of the W pair cross-section

The sensitivity of the threshold cross-section to the W mass comes from processes with two resonant Ws, represented by the so-called CC03 diagrams in Fig. 1a, which lead to a four-fermion final state. Many other diagrams, such as those in Fig. 1b, lead to the same four-fermion final states and interfere with the CC03 diagrams. The contribution of these diagrams to the total cross-section can be very large, in particular for final states containing electrons or fermion-antifermion pairs; however, their effect reduces to at most a few percent by requiring that all four fermions be within detector acceptance and well separated from each other. Therefore the selection procedures were optimized for the CC03 processes and results presented as CC03 cross-sections. The effect of the other diagrams is corrected for by comparing Monte Carlo simulations including a) only CC03 processes and b) the full set of four-fermion diagrams.

Two Monte Carlo event generators were used to simulate the signal events, i.e., four-fermion final states which can come from WW production and decay.

- KORALW, version 1.21 [12]. This program includes multi-photon initial state radiation with finite photon transverse momentum via Yennie-Frautschi-Suura exponentiation [14], final state radiation via PHOTOS [13], and Coulomb correction [15]. It can generate CC03 diagrams only, or include four-fermion diagrams computed with the GRACE package [16], with fixed W and Z widths. The JETSET [17] package takes care of gluon radiation and hadronization; no colour reconnection [18] effects are included. In four-quark final states the colour flow is chosen with probabilities proportional to the matrix elements squared for WW and ZZ production [20]. Samples of 10,000 events were generated with W masses of 79.75, 80.25 and 80.75 GeV/c^2, both for CC03 diagrams only and for all four-fermion diagrams. In this last case, loose cuts were applied at the generation level on the outgoing electron angle or the fermion-antifermion pair invariant masses, avoiding regions of phase space with poles in the cross-section. Signal events produced in these regions would anyway be rejected by the selection cuts.
- For comparison, the EXCALIBUR [21] generator was used. It includes initial state radiation collinear with the beams [22], final state radiation via PHOTOS [13],

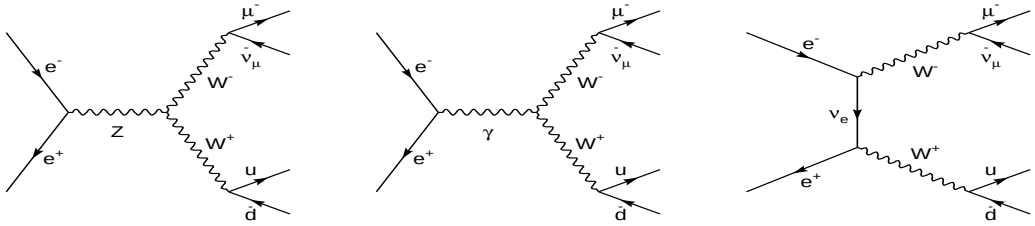

(a) The CC03 diagrams (in this example, $\mathrm{e^+e^-} \to \mu^- \bar{\nu}_\mu \mathrm{u\bar{d}}$).

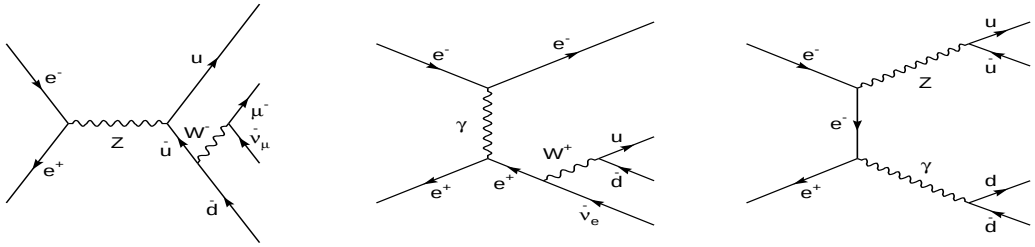

(b) Three important four-fermion diagrams which interfere with the CC03 processes.

Figure 1: Examples of CC03 and four-fermion diagrams.

Coulomb correction [15] and hadronization by JETSET [17]. A comparison sample was generated with $m_{\mathrm{W}} = 80.25\ \mathrm{GeV}/c^2$ and the same choice of colour flow as above. For the second sample, the same events were hadronized following the colour reconnection Ansatz of [19]. Here also, loose cuts were applied at the generation level.

The KORALW samples with $m_{\mathrm{W}} = 80.25\ \mathrm{GeV}/c^2$ serve to determine the efficiencies used to obtain the central value of the final result. The other samples are used to check the m_{W} dependence of the selection procedures and of the four-fermion to CC03 correction. The EXCALIBUR samples are used as a cross-check of the Monte Carlo simulation of the physics processes, and to assess the effects of colour reconnection.

Monte Carlo samples corresponding to integrated luminosities at least twenty times as large as that of the data were fully simulated for all background reactions. Annihilation into quark pairs, $\mathrm{e^+e^-} \to \mathrm{q\overline{q}}(\gamma)$, was simulated with PYTHIA [17]. Two-photon ($\gamma\gamma$) reactions into leptons and hadrons were simulated with the PHOT02 [23] and PYTHIA generators. KORALZ [24] and UNIBAB [25] were used for dilepton final states. Finally, PYTHIA and FERMISV [26] were used for various processes leading to four-fermion final states. Where appropriate, results from the two programs were cross-checked against each other. To avoid double-counting of four-fermion events between the signal and background Monte Carlos, events with a flavour content that could originate from WW production were explicitly rejected from the background samples.

To extract the cross-section the analysis proceeds as follows.

- The number N_{obs} of events observed after a given selection is determined.
- The number N_{back} of events expected from background processes leading to final states inconsistent with WW production is subtracted.

– The contribution from four-fermion diagrams other than CC03, but with final states consistent with WW production, is estimated as

$$N_{4f}^{\overline{\mathrm{CC03}}} = \mathcal{L}\left[\varepsilon_{4f}\sigma_{4f}^{\mathrm{MC}} - \varepsilon_{\mathrm{CC03}}\sigma_{\mathrm{CC03}}^{\mathrm{MC}}\right], \tag{1}$$

where ε_{4f} and $\varepsilon_{\mathrm{CC03}}$ are the selection efficiencies obtained with the full four-fermion and the CC03 Monte Carlo samples, $\sigma_{4f}^{\mathrm{MC}}$ and $\sigma_{\mathrm{CC03}}^{\mathrm{MC}}$ are the corresponding generated cross-sections, and $\mathcal{L}$ is the total luminosity analyzed. Although ε_{4f} and $\sigma_{4f}^{\mathrm{MC}}$ depend on the loose cuts applied at generation level, the product $\varepsilon_{4f}\sigma_{4f}^{\mathrm{MC}}$ does not. This contribution is subtracted from N_{obs} as well.

– Finally, the CC03 cross-section is obtained as

$$\sigma_{\mathrm{CC03}} = \frac{N_{obs} - N_{back} - N_{4f}^{\overline{\mathrm{CC03}}}}{\mathcal{L}\,\varepsilon_{\mathrm{CC03}}}\,. \tag{2}$$

Hereafter, the quantity $N_{4f}^{\overline{\mathrm{CC03}}}/\mathcal{L}\,\varepsilon_{\mathrm{CC03}}$ is called four-fermion to CC03 correction. This procedure renders the CC03 result insensitive to the value of the W mass used in the Monte Carlo generation. It is, however, only an approximation since the effect of interfering diagrams is treated like a background subtraction. Correcting by the ratio instead of the difference of Monte Carlo predictions would give the same results within one percent, while not correcting at all for the non-CC03 diagrams would lead to a difference of several percent. The CC03 efficiency does not depend on generation cuts and provides a direct indication of the effectiveness of the analyses in selecting those signal events which are most sensitive to the W mass. For this reason, unless explicitly stated, the signal efficiencies quoted in the following are CC03 efficiencies.

4 Selection of W pair candidates

4.1 $\mathrm{W^+W^-} \to \ell^+\nu\ell^-\bar{\nu}$ events

The fully leptonic channel is characterized by two acoplanar energetic leptons and large missing momentum carried away by the corresponding neutrinos. As Ws are produced with low velocity at threshold, the typical momentum of these primary leptons lies in a relatively narrow range around 40 GeV/c. It is expected that in 5/9 of the events, at least one of the two leptons is a tau; in this case, the tau decays give rise to softer final states, possibly a thin hadronic jet, and more momentum is carried away by the additional neutrinos.

Two selections for the $\mathrm{W^+W^-} \to \ell^+\nu\ell^-\bar{\nu}$ signal were developed. They have similar overall efficiencies (62.7% and 66.9%) and background levels (0.038 pb and 0.028 pb), but differ in their sensitivities to the individual dilepton channels. The first analysis is based on topological information and is sensitive to all channels. The second analysis requires the presence of at least one high momentum electron or muon, identified using the standard ALEPH algorithms [9]. This leads to a comparatively lower efficiency (24% instead of 48%) for events where both Ws decay to taus. The efficiency is higher in all other channels, since backgrounds featuring a high momentum electron or muon have better defined kinematics, and can be eliminated with less stringent cuts. Events are accepted as WW candidates if they pass either of the two selections. The combined efficiency is 74%, for a background of 0.053 pb.

Details of the two analyses are given now. Both require a low multiplicity of good tracks. In the first selection, events are accepted if they contain two or four good tracks with zero total electric charge. The four-track case is reduced to a two-jet topology by merging the three tracks with the smallest invariant mass. This triplet is interpreted as coming from a three-prong tau decay, and its mass is required to be smaller than 1.5 GeV/c^2. In the second analysis, events with any number of good tracks between two and six are kept; all energy-flow particles are then clustered into jets by the JADE [27] algorithm at a y_{cut} of 0.002, and events with two or three jets are kept, provided that the identified lepton is the only charged particle in its jet.

Both analyses apply photon vetoes against radiative dilepton events. In the first selection, events are rejected if there is an isolated neutral energy flow particle of more than 1 GeV outside a cone of 10° around each jet and forming an invariant mass with each of them of more than 2 GeV/c^2. In the second analysis, three-jet events are rejected unless the least energetic jet has an energy lower than 5 GeV and is made only of neutral particles. To further reject radiative dileptons and two-photon events, both selections require that no energy be found in a cone of 12° around the beam axis. The backgrounds from two-photon and non-WW four-fermion processes are reduced further by requiring a visible invariant mass in excess of 12 GeV/c^2. The first selection requires a missing transverse momentum larger than $0.030\sqrt{s}$ and an acoplanarity lower than 170°. These cuts are looser in the second selection, $0.025\sqrt{s}$ and 174°, respectively. Fig. 2 shows the acoplanarity distribution at this stage of the selection, for the second analysis.

Further cuts are applied to reduce the background from $\gamma\gamma \to \tau^+\tau^-$ events. In the first analysis, the jet momenta are projected into the plane transverse to the beam axis and the 2D-thrust axis is built from these projections. The scalar sum of their transverse components with respect to the 2D-thrust axis is required to be greater than 2 GeV/c. Similarly, the second analysis applies a combined cut on acollinearity and on the transverse component of the missing momentum with respect to the plane defined by the beam axis and the 3D-thrust axis, $\not\!\!p_T^{out}$: events are accepted either if $\not\!\!p_T^{out}$ is greater than 2 GeV/c, or if the acollinearity is lower than 110°. Finally, the second analysis requires that the energy of the most energetic jet lies between 28 and 55 GeV.

In the data, six events pass either selection, in fact they all pass both. The residual background amounts to 0.6 events and is dominated by $\gamma\gamma \to \tau\tau$ and four-fermion events (mainly $\gamma^*\mathrm{Z} \to \ell^+\ell^-\nu_{\ell'}\bar{\nu}_{\ell'}$, with $\ell \neq \ell'$, the case $\ell = \ell'$ being part of the signal). The four-fermion background was calculated with the FERMISV Monte Carlo to be 0.013 ± 0.009 pb, where the systematic error was assigned by comparing the results to those of PYTHIA and EXCALIBUR. The largest detector-related systematic effects come from the photon vetoes. Events triggered at random beam crossings were used to assess the losses due to beam related background and electronic noise. The effect of photon vetoes was estimated to cause a loss of efficiency of 4%, with a systematic uncertainty of ±2%. The overall systematic error amounts to ±0.029 pb and is dominated by Monte Carlo statistics.

The four-fermion to CC03 correction amounts to -0.014 pb, giving

$$\sigma_{\mathrm{CC03}}(\mathrm{WW} \to \ell^+\nu\ell^-\bar{\nu}) = 0.68^{+0.34}_{-0.26}\,(\mathrm{stat.})\ \pm 0.03\,(\mathrm{syst.})\,\mathrm{pb}. \qquad (3)$$

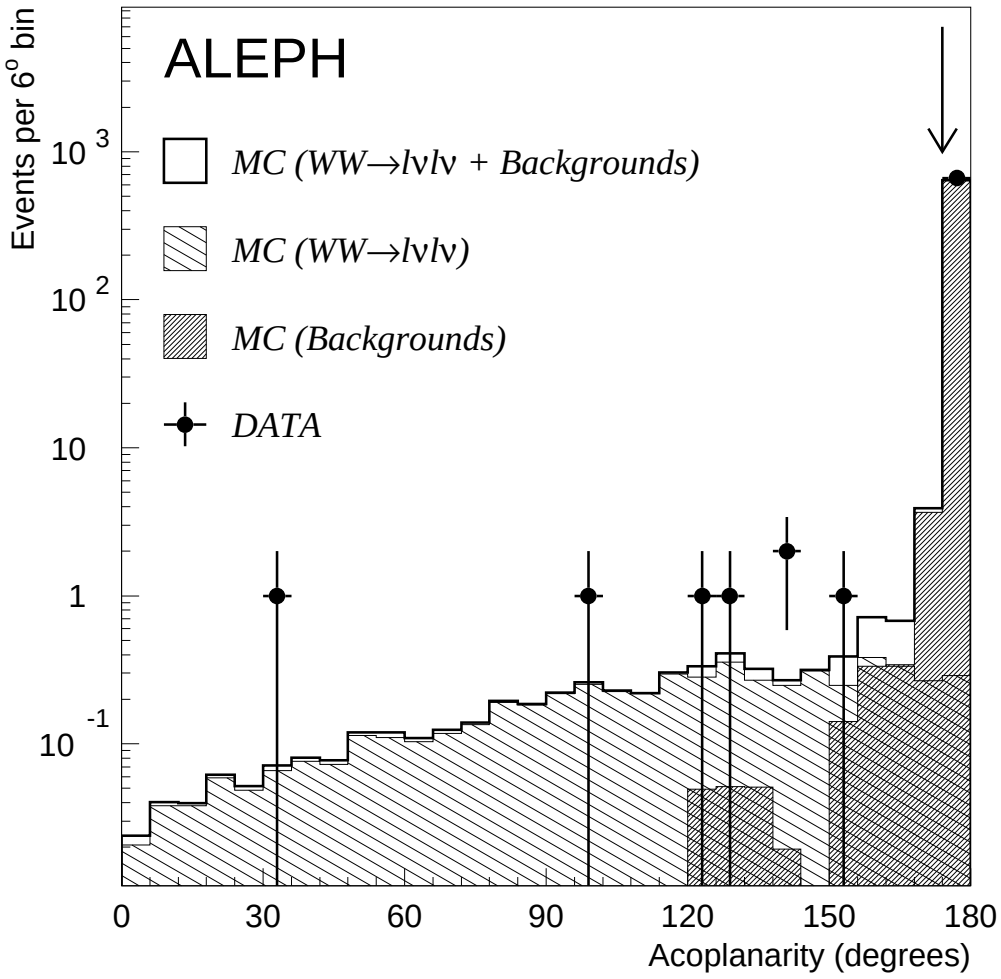

Figure 2: *The acoplanarity distribution in the second* $\mathrm{W^+W^-} \to \ell^+\nu\ell^-\bar{\nu}$ *analysis, after all cuts except those on acoplanarity (indicated here by the arrow), acollinearity,* $\not{p}_T^{out}$ *and jet energy. The MC expectation for the signal is normalized to the measured cross-section.*

4.2 $\mathrm{W^+W^-} \to \ell\nu\mathrm{q\overline{q}}$ events

The typical final state for semileptonic WW events at threshold consists of a lepton of energy about 40 GeV, large missing momentum from the neutrino, and two hadronic jets of energy also close to 40 GeV. An example is shown in Fig. 3.

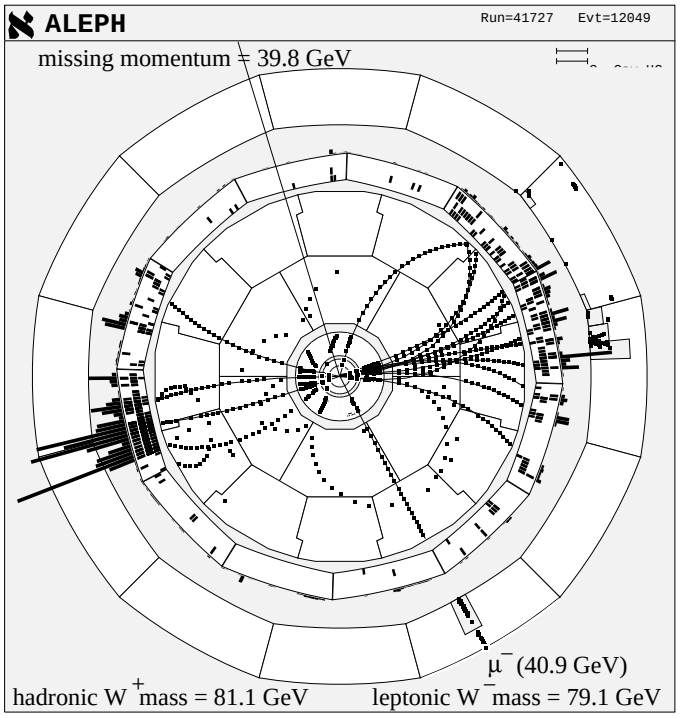

Figure 3: *An event with a W pair decaying to* $\mu\nu\mathrm{q\overline{q}}$.

In one third of the cases, when the lepton is a τ, additional energy and momentum are lost in neutrinos from its decay. In all channels, the lepton (or the thin jet from the τ decay) points in a direction roughly opposite the missing momentum and is generally well separated from the two hadronic jets, which are also approximately back-to-back. Three selection procedures were developed. As in the previous section, one selection is optimized for WW events with electrons or muons and requires an energetic identified electron or muon, the other two were developed for $\tau\nu\mathrm{q\overline{q}}$ events, based on global variables or topological properties of events.

4.2.1 $\mathrm{WW} \to \mathrm{e}\nu\mathrm{q\overline{q}}$ *and* $\mathrm{WW} \to \mu\nu\mathrm{q\overline{q}}$ *selections*

In this analysis, a loose preselection is first applied based on variables for which signal and background distributions are very different; at least five good tracks are required, with a total charged energy greater than $0.12\sqrt{s}$. The missing 4-momentum ($\not\!\!E$, $\not\!\!p$) is used to reduce the non-radiative $\mathrm{q\overline{q}}$ background and remove most of the radiative component. All good tracks with momentum greater than 1 GeV/c are then projected onto the direction of the missing momentum and the track with the highest momentum antiparallel to the missing momentum is chosen as the lepton candidate. In most of the $\mathrm{q\overline{q}}$ events, a random fragmentation charged particle is selected, while in signal events the correct high energy lepton from a W decay is chosen. Therefore requiring loose electron or muon identification

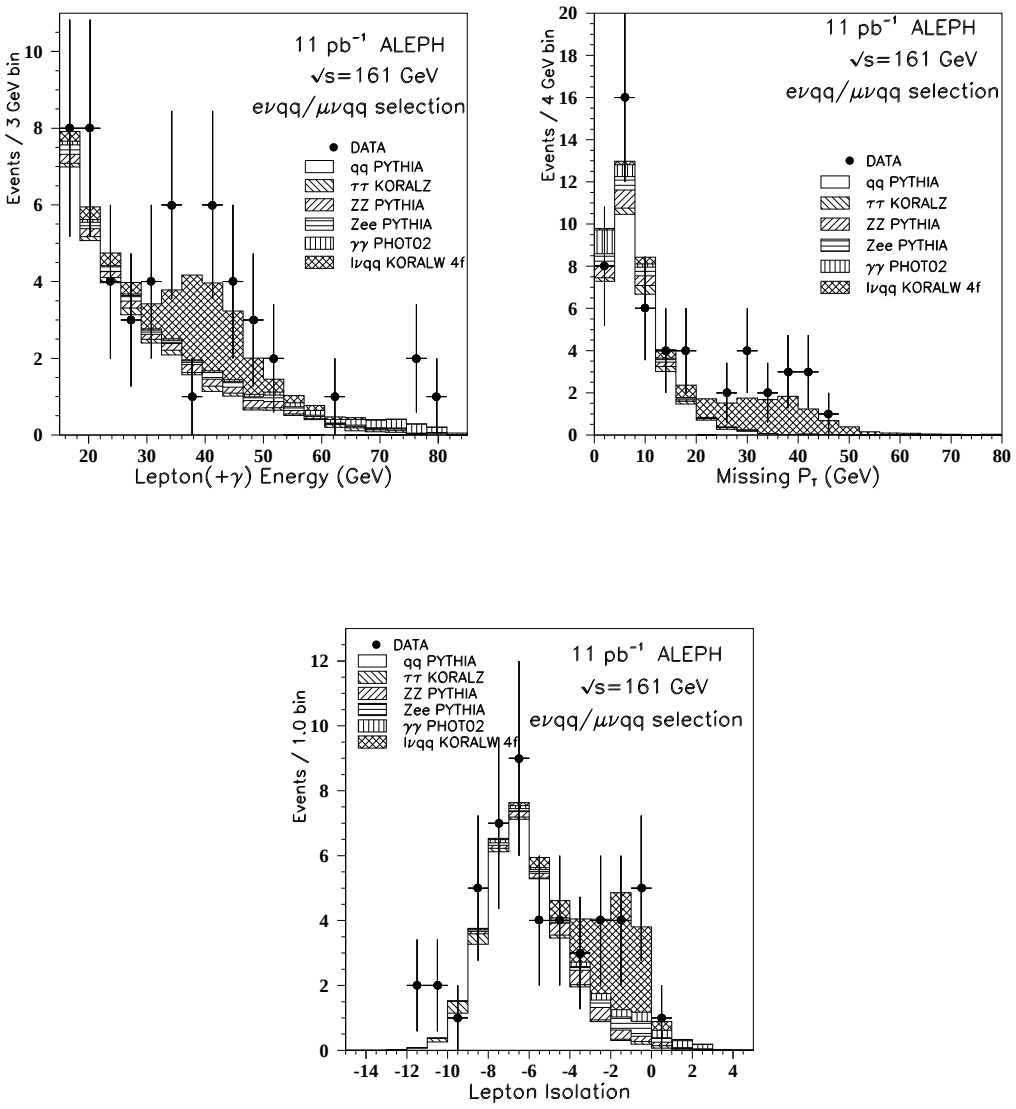

Figure 4: *Properties of $\ell\nu q\bar{q}$ events after preselection. (a) Lepton energy distribution; (b) Missing transverse momentum; (c) Lepton isolation.*

criteria and an energy of at least 15 GeV for the lepton candidate rejects most background events. For electrons the energy is corrected for possible Bremsstrahlung photons detected in the electromagnetic calorimeter. The remaining particles are clustered into two jets with the Durham [28] algorithm.

After this preselection, the probability for an event to come from the signal process is built from Monte Carlo samples of signal and backgrounds as follows. The following three variables, shown in Fig. 4, define a three-dimensional space: i) the energy of the lepton; ii) the total missing transverse momentum; iii) the lepton isolation, defined as

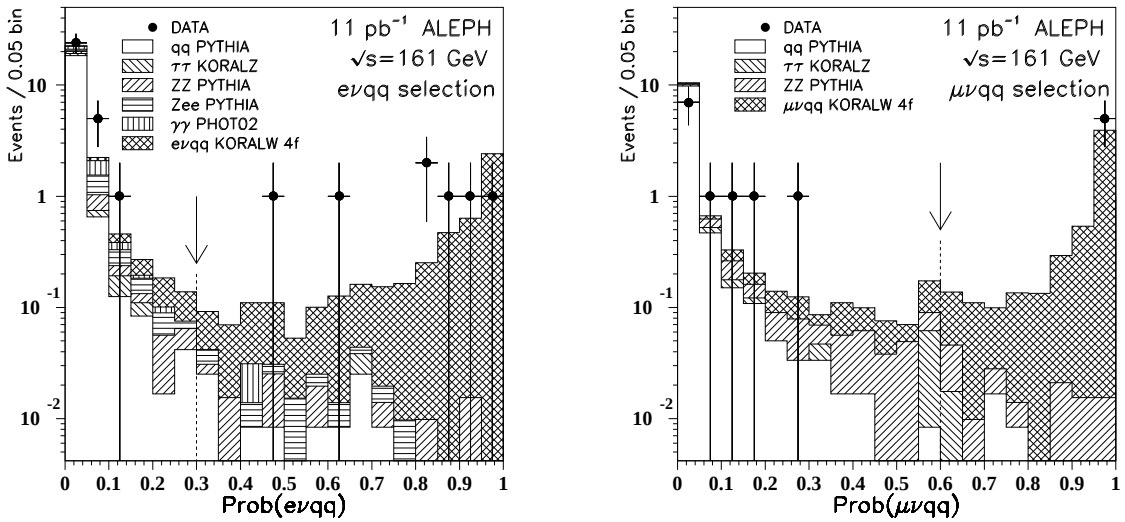

Figure 5: *Probability distribution of preselected ALEPH events for the* $\mathrm{e}\nu\mathrm{q}\overline{\mathrm{q}}$ *and the* $\mu\nu\mathrm{q}\overline{\mathrm{q}}$ *selections. Vertical axis: number of events per bin in the data.*

$\log(\tan\theta_{\mathrm{Jet}}/2) + \log(\tan\theta_{\mathrm{Chg}}/2)$, where θ_{Jet} and θ_{Chg} are, respectively, the smallest angle between the lepton and any hadronic jet, and the smallest angle between the lepton and any good track. Given a data point in this 3D-space, the luminosity-normalized probability density function (p.d.f.) is estimated as the density in the smallest cube, centred on the data point, that contains $\sqrt{N}$ preselected MC events [29], where N is the total number of preselected Monte Carlo events. This is done separately for signal and backgrounds. The probability for the data event to be signal is then the ratio of the signal p.d.f. to the sum of the signal and background p.d.f.

Events are selected if they have a probability larger than 0.30 to be an $\mathrm{e}\nu\mathrm{q}\overline{\mathrm{q}}$ event, or a probability larger than 0.60 to be a $\mu\nu\mathrm{q}\overline{\mathrm{q}}$ event. These cuts were designed, from Monte Carlo studies, to minimize the statistical error on the W mass. The final probability distributions of preselected $\mathrm{e}\nu\mathrm{q}\overline{\mathrm{q}}$ and $\mu\nu\mathrm{q}\overline{\mathrm{q}}$ Monte Carlo and data candidates are shown in Fig. 5. With these cuts, the selection efficiencies are 83.4% and 87.9%, for $\mathrm{e}\nu\mathrm{q}\overline{\mathrm{q}}$ and $\mu\nu\mathrm{q}\overline{\mathrm{q}}$, on a total background of 0.034 pb.

4.2.2 $\mathrm{WW} \to \tau\nu\mathrm{q}\overline{\mathrm{q}}$ *events*

The analysis optimized for the selection of $\mathrm{WW} \to \tau\nu\mathrm{q}\overline{\mathrm{q}}$ events is based on two complementary approaches: the global selection cuts on global variables of the event, such as acollinearity and acoplanarity, while the topological selection attempts to identify the tau jet. The inclusive combination of these two selections has an efficiency of 49.9% in the $\mathrm{WW} \to \tau\nu\mathrm{q}\overline{\mathrm{q}}$ channel, with a background of 0.053 pb.

The preselection is common to the two analyses. A minimum of seven good tracks is required. The energy found in a cone of 12° around the beam axis must be less than $0.025\sqrt{s}$, and the polar angle of the missing momentum must be greater than $25.8°$. In order to suppress radiative events with large-angle photons, events containing an identified photon of energy

greater than 10 GeV, isolated from other particles by more than 30°, are rejected.

The global selection relies on the fact that semileptonic events are acollinear and acoplanar. The event is divided into two hemispheres by the plane perpendicular to the thrust axis; acollinearity and acoplanarity, calculated from the directions of the total momenta of all particles in the two hemispheres, are required to be less than 165° and 170° respectively. The missing momentum should be isolated in space and in the transverse plane; the energy contained in an azimuthal wedge of half-angle 30° with respect to the plane defined by the beam and the missing momentum directions is required to be less than $0.10\sqrt{s}$. Moreover, the energy in a cone of half angle 20° around the direction of the missing momentum is required to be less than $0.025\sqrt{s}$. In order to reduce the contribution from single W production the energy of the primary ν_τ, estimated as $E_{\nu_\tau} = \frac{1}{2}(\not{p} + \not{E})$, is required to be less than 50 GeV and the missing mass is required to be less than 70 GeV/c^2.

In the topological selection, jets are reconstructed with the JADE algorithm, using a y_{cut} of 0.001. A minimum of three jets should be found. Jets containing only one good track and with a charged momentum greater than 4 GeV/c are identified as tau-jet candidates; any remaining ambiguity is resolved by chosing the jet closest to being opposite to the missing momentum. All other jets are merged into two jets, which will be referred to as quark-jets in the following. In order to reduce the $\mathrm{q\overline{q}}(\gamma)$ background, the tau-jet must be separated by more than 25° from the the other jets, no quark-jet must have an energy larger than 50 GeV, and the invariant mass of the quark-jets must be greater than 60 GeV/c^2. The interfering background from single W production, where the W generally has a large boost, is removed by requiring that the acollinearity of the quark-jets is greater than 130°.

4.2.3 Combined results for the semileptonic channels

The three analyses are combined inclusively. A total of 16 events are selected, of which 7 have a high energy identified electron, 5 have a high energy identified muon, and 4 are likely to contain a tau. The combined efficiency is 87.1% for the electron channel, 90.1% for muons, 51.4% for taus, and 76.1% overall.

The background, calculated with the PYTHIA Monte Carlo, amounts to 0.084 pb; it is dominated by $\mathrm{q\overline{q}}$, ZZ^* and $\mathrm{Ze^+e^-}$events. A systematic error of $\pm$0.015 pb was assigned by summing the following contributions: i) Monte Carlo statistics; ii) $\mathrm{q\overline{q}}$ modelling, assessed by the deviations of Monte Carlo from LEP1 data, using the same selections with cuts rescaled by the ratio of centre-of-mass energies; iii) comparison of the normalization and distributions of preselected Monte Carlo and data candidates with signal probabilities smaller than 0.10; iv) overall normalization of the $\mathrm{q\overline{q}}$ background, assessed using radiative returns to the Z peak. Systematic errors on signal efficiencies are evaluated to be $\pm$2.4%, coming from i) Monte Carlo statistics, ii) detector-related systematic effects such as errors from the photon vetoes, and iii) uncertainties in the lepton identification, assessed by the agreement between LEP1 data and Monte Carlo for dilepton events.

In this channel, the four-fermion processes interfere negatively and the four-fermion to CC03 correction is +0.051 pb. An uncertainty of $\pm$0.015 pb was assigned to this correction, accounting for Monte Carlo statistics and changes in the correction when varying m_{W} in the 79.75–80.75 GeV/c^2 range. The resulting cross-section for the semileptonic WW channel is:

$$\sigma_{\mathrm{CC03}}(\mathrm{WW} \to \ell\nu\mathrm{q\overline{q}}) = 1.85^{+0.51}_{-0.43}(\mathrm{stat.}) \pm 0.06(\mathrm{syst.})\mathrm{pb}. \quad (4)$$

4.3 $\mathrm{W^+W^-} \to \mathrm{q\overline{q}q\overline{q}}$ events

These events feature no missing energy and must be separated statistically from the main background coming from $\mathrm{e^+e^-} \to \mathrm{q\overline{q}} \to \mathrm{multijets}$. Four different methods have been used. Each of these uses a simple preselection, followed by a multivariable analysis to determine the cross-section. The four multivariable methods employed are: (1) a linear discriminant analysis, (2) a neural network, (3) a rarity analysis and (4) a weighting technique. Each of these is described below. The four-fermion to CC03 correction is typically -0.14 pb for all methods. The background contributions were evaluated by Monte Carlo and normalized to the analyzed luminosity.

4.3.1 Preselection

A large fraction of the backgrounds, in particular $\mathrm{q\overline{q}}$ events with large initial state radiation, can be eliminated with simple preselection cuts, while maintaining a high efficiency for the signal. For example, the preselection cuts applied by the rarity analysis are: (i) total visible energy > 120 GeV and missing momentum $< 30\ \mathrm{GeV}/c$; (ii) at least 43 energy-flow particles, 21 of which must be charged; (iii) at least four jets found using the JADE algorithm with $y_{cut} = 0.005$. The remaining events are forced to form four jets using the Durham [28] algorithm and the following further cuts are applied: (iv) at least four particles per jet, with at least one good track; (v) sum of the cosines of the six possible angles between the four jets < -1; (vi) $\log y_{34} > -6$, where y_{34} is the value of y_{cut} at which the transition from three to four jets occurs. The performance of this preselection are summarized in Table 1, along with those of the other three analyses.

After preselection, a set of distributions in which WW events are statistically different from backgrounds is shown in Fig. 6. It is clear that selection on a single distribution is not sufficient to extract a significant signal, while a series of cuts would lead to unacceptable loss of efficiency.

Analysis	data	Monte Carlo	efficiency(%)	signal/background
Discriminant Analysis	70	69.4	83.0	0.28
Neural Net	111	95.0	90.9	0.21
Rarity	80	78.5	90.5	0.27
Weights	262	275.2	93.9	0.08

Table 1: *The number of events preselected by each hadronic analysis is compared with the total number predicted by signal and background Monte Carlo. The efficiency of the preselection for* $\mathrm{W^+W^-} \to \mathrm{q\overline{q}q\overline{q}}$ *and the resulting signal/background ratio are also shown.*

4.3.2 Linear discriminant analysis

In this method, a single discriminating variable, U, is built from a linear combination of several variables. This is done by first ordering the variables by their individual power to discriminate between the signal and the background. Starting with the most discriminating one, the variables are added one by one to a linear combination of maximum discriminating power. For this analysis, the six most discriminating variables were i) the Durham algorithm y_{34}; ii) the minimum jet energy; iii) the sum of the cosines of the angles between all pairings

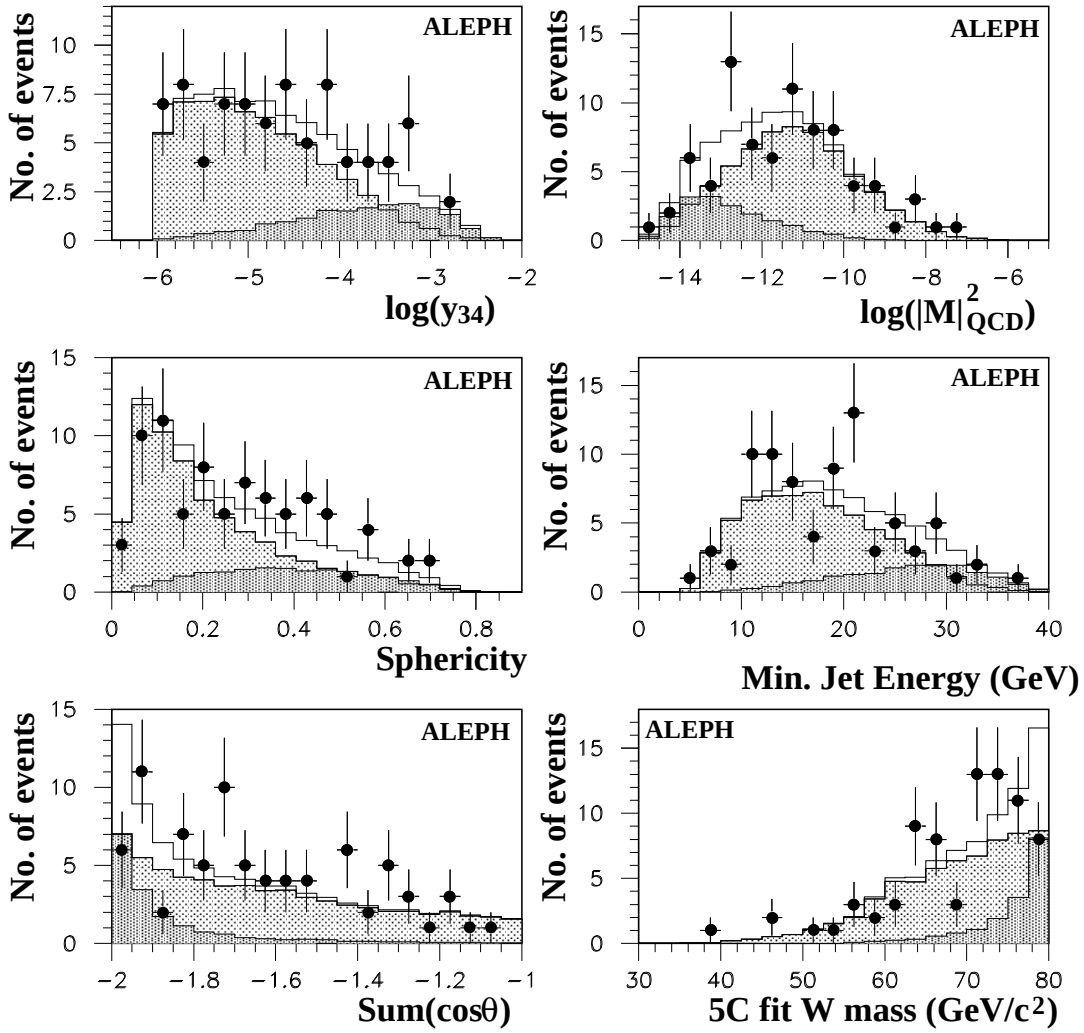

Figure 6: *Distributions of four jet events after preselection (here from the rarity method). The points with error bars are the data, and the open histograms, the Monte Carlo. The dark shadowed histograms show the contribution from signal, and the light shadowed histograms the contribution from backgrounds.*

of jets; iv) the largest QCD matrix element squared of all jet permutations for $\mathrm{e^+e^-} \to 4\,\mathrm{jets}$ through a virtual Z or γ; v) the event sphericity; and vi) the WW matrix element squared for $\mathrm{e^+e^-} \to \mathrm{WW} \to 4\,\mathrm{jets}$.

A comparison between data and Monte Carlo for the optimal linear combination U is shown in Fig. 7a. A Monte Carlo study has shown that the maximum sensitivity to m_{W} is achieved by cutting at $U \geq 0$, yielding an efficiency of 60%. This selects 16 events in the data on an expected non-WW background of 5.5 events. The resulting cross-section is $\sigma^{\mathrm{disc}}_{\mathrm{CC03}} = 1.60 \pm 0.58$ pb.

4.3.3 Neural Network

In this analysis, a feed-forward layered neural network trained with back-propagation is used to distinguish between the WW signal and the background. The neural network essentially builds the multidimensional p.d.f. for both signal and background, and gives as output an estimate of the probability for a given event to be signal or background [30]. Nine input variables were used: the Durham algorithm y_{34}; y_{23} – similar to y_{34} for the two-to-three jet transition; minimum invariant mass between any two jets; sphericity; aplanarity; acollinearity; thrust; QCD matrix element squared; minimum jet energy. The neural network output distribution is shown in Fig. 7b for all events passing the preselection. The hadronic WW cross-section, extracted by a binned log-likelihood fit to this distribution, is: $\sigma^{\mathrm{NN}}_{\mathrm{CC03}} = 1.93\ ^{+0.66}_{-0.57}$ pb.

4.3.4 Rarity

In the rarity method [31], for each event i, variables x^i_j are first constructed such that they take low values for the $\mathrm{q\overline{q}}$ background and high values for the WW signal. A new variable T_i is built, which is the fraction of WW Monte Carlo events for which $x_j \leq x^i_j$ for all variables x_j. The rarity R_i is then the integral probability of T_i, namely the fraction of WW Monte Carlo events for which $T \leq T_i$. The rarity distribution is, by construction, flat between 0 and 1 for the WW signal, and peaked around 0 for the background. Six variables were combined in this way: the Durham algorithm y_{34}; QCD matrix element squared; sphericity; minimum jet energy; sum of the cosines of the angles between all pairings of jets; and average fit mass of jet pairs. The resulting rarity distribution is shown in Fig. 7c. The cross-section, determined by a likelihood fit to this distribution, is $\sigma^{\mathrm{rar}}_{\mathrm{CC03}} = 1.92\ ^{+0.59}_{-0.60}$ pb.

4.3.5 Weights

In this method, each preselected event is weighted according to its location in a binned multidimensional space of discriminating variables [32]. The weight in each bin, $g(x)$, is estimated from the Monte Carlo sample including signal and all backgrounds as the fraction of WW events in that bin. The cross-section is then evaluated using Eq. 1 and 2 by making the following replacements:

$$N_{obs} \leftrightarrow \sum_{\mathrm{data}} g(x)\ ;\ \ N_{back} \leftrightarrow \sum_{\mathrm{bkgd\ MC}} g(x)\ ;\ \ \mathcal{L}.\varepsilon.\sigma^{\mathrm{MC}} \leftrightarrow \sum_{\mathrm{WW\ MC}} g(x)\ ,$$

where the sums run over individual events in the data or in the background or WW Monte Carlo samples. The Monte Carlo sums are normalized to the analyzed luminosity. The last term is calculated for both four-fermion and CC03 Monte Carlo samples. The statistical error was calculated according to Ref. [32]. Five variables were used: average fit mass of jet pairs; JADE y_{34}; sphericity; sum of transverse momenta squared of particles with respect to their jets; minimum jet energy. The distribution of weights for the preselected events is shown in Fig. 7d, compared with Monte Carlo expectations. The CC03 cross-section is: $\sigma^{\mathrm{weights}}_{\mathrm{CC03}} = 1.79 \pm 0.53$ pb.

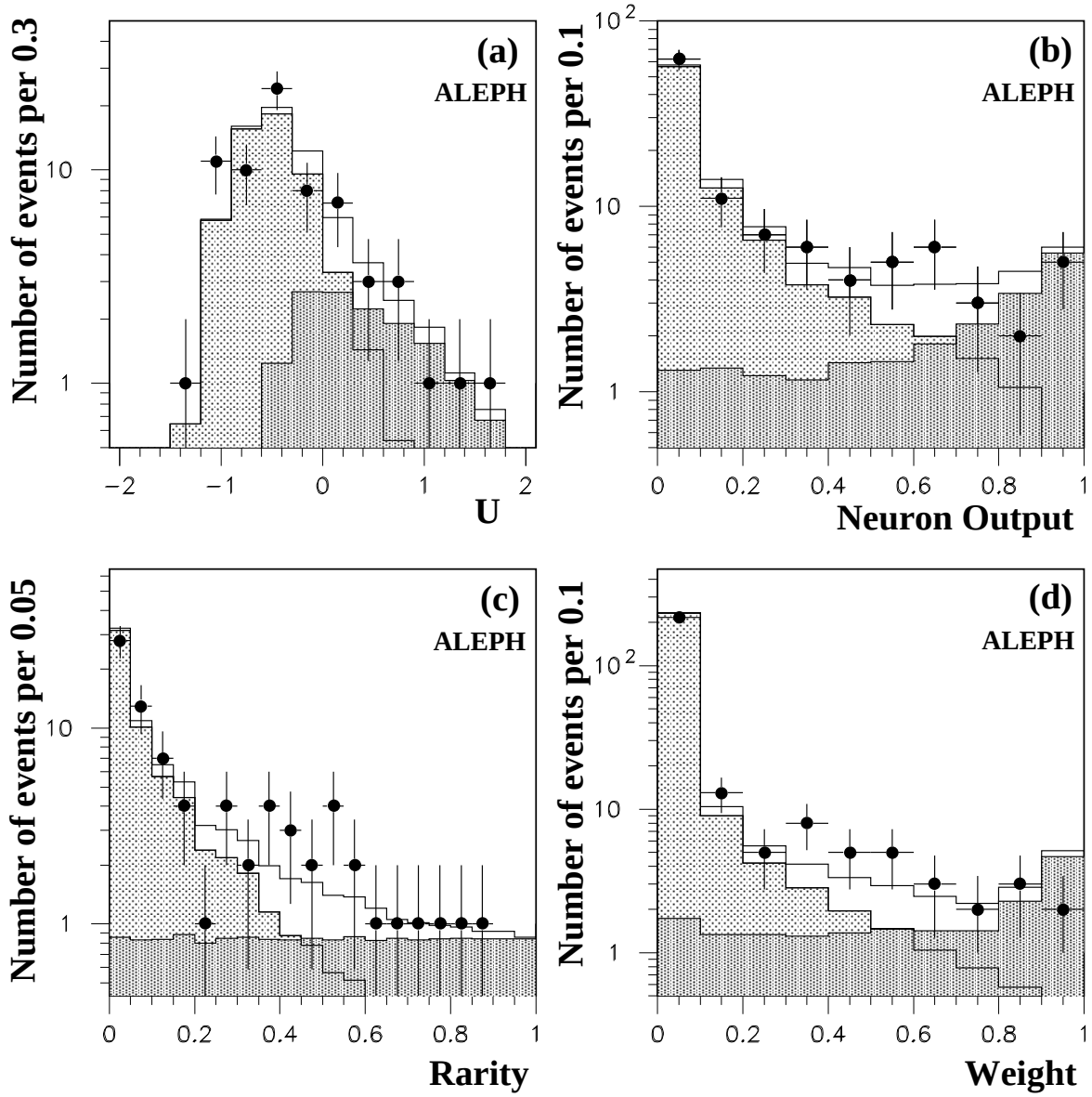

Figure 7: *Comparison between data and Monte Carlo after preselection for (a) the discriminant variable U, (b) the neural network output distribution, (c) the rarity distribution and (d) the weight distribution. The points are the data, the open histogram the total Monte Carlo prediction. The light shadowed histogram shows the expected background and the dark shadowed histogram the expected* $\mathrm{WW} \to \mathrm{q\overline{q}q\overline{q}}$ *contribution for* $m_{\mathrm{W}} = 80.25\ \mathrm{GeV}/c^2$.

4.3.6 Systematic errors

The following sources of systematic errors were considered.

- The preselection error was determined by modifying the distributions of the variables used from the Monte Carlo to match those of the data and then re-running the analysis. The difference in the result is assigned as the error.
- The errors resulting from the particular Monte Carlo generators used were estimated by using alternative generators, EXCALIBUR for the WW signal, HERWIG [33] for the $\mathrm{q\overline{q}}$ background. In addition, an uncertainty of 5% was applied to the normalization of the background estimated from the data/Monte Carlo agreement in the rate of low weight events and from comparison of four jet rates in hadronic Z decays.
- The effect of colour recombination and Bose-Einstein correlations are both expected to be small as they would only produce small changes in the distributions of certain variables, e.g. the fitted mass, and not directly affect the WW cross-section [18]. Nevertheless, the effect of colour recombination was estimated by comparing the results produced by versions of EXCALIBUR with and without its implementation. The difference is found to be less than 0.03 pb. A similar error is expected from Bose-Einstein correlations.
- Systematic errors arising from possible inaccuracies in the simulation of the variables used in the multivariate analysis were determined by using different combinations of these variables in the analysis. The variation in the resulting cross-sections is larger than, though statistically consistent with, that expected from 50 Monte Carlo samples. The difference of 0.11 pb between these scatters was assigned as the systematic error.
- An estimate of the effect of the largest possible detector miscalibrations led to negligible values.
- Monte Carlo statistics and luminosity uncertainty lead to cross-section uncertainties of 0.03 pb and 0.02 pb, respectively.

For each of these sources of systematic errors, evaluations varied slightly between the different analyses. In each case the most pessimistic evaluation was kept. The components of the systematic error, summarized in Table 2, were added in quadrature to obtain a total systematic error of 0.19 pb.

Source	Error (pb)
Preselection	0.09
B.E. and colour recombination	0.03
QCD normalization	0.07
QCD generator	0.09
Choice of discriminating variables	0.11
MC statistics	0.03
Luminosity	0.02
Total (in quadrature)	0.19

Table 2: *Contributions to the systematic error on the cross-section for* $\mathrm{WW} \to \mathrm{q\overline{q}q\overline{q}}$.

4.3.7 Combination of the methods

The expected differences and correlations between the four methods described above were obtained by applying them on 100 independent Monte Carlo samples, each corresponding to 11.1 pb^{-1}. The spread of the 100 cross-section results were found to be of similar size for the four analyses, and statistically consistent with the errors calculated for the data. The correlations were found to range from 0.66 to 0.85. The four methods give consistent results, but none of them achieved maximum efficiency. It is therefore worthwhile to combine them. This was done using the technique of Lyons et al. [34], in which a weighted average was built, taking into account the covariance matrix calculated from the Monte Carlo study.

The combined cross-section for the hadronic channel is finally:

$$\sigma_{\mathrm{CC03}}(\mathrm{WW} \to \mathrm{q\overline{q}q\overline{q}}) = 1.80 \pm 0.50\ (\mathrm{stat}) \pm 0.19\ (\mathrm{syst})\ \mathrm{pb}. \tag{5}$$

5 W pair cross-section and W mass

The results from the three channels were combined assuming the Standard Model branching ratios. A maximum likelihood method was performed, using as input the measured number of events in the lepton-lepton and lepton-hadron channels and the combined cross-section for the hadron-hadron channel. The CC03 cross-section is

$$\sigma_{\mathrm{WW}} = 4.23 \pm 0.73 \pm 0.19\ \mathrm{pb}\ , \tag{6}$$

where the first error is statistical and the second, systematic, is dominated by the uncertainties in the $\mathrm{q\overline{q}q\overline{q}}$ channel. The result obtained by summing the individual cross-sections is very similar. The result is in good agreement with the expected cross-section, which is 3.77 ± 0.27 pb for the current world average value, $m_{\mathrm{W}} = 80.356 \pm 0.125\ \mathrm{GeV}/c^2$ [4]. The additional variation upon the Higgs boson mass amounts to ± 0.02 pb [5]. If the measured cross-section were exactly equal to the expected one, the statistical error would be 0.71 pb. This error is to be used in the combination with other experiments.

The W mass was obtained, within the framework of the Standard Model, from σ_{WW} using the program `GENTLE` [35]. The result is

$$m_{\mathrm{W}} = 80.14 \pm 0.34 \pm 0.09 \pm 0.03(\mathrm{LEP})\ \mathrm{GeV}/c^2, \tag{7}$$

where the first error is statistical and the second comes from systematic errors in the cross-section. As for the Z, this mass corresponds to the convention where the propagator includes a s-dependent width. The last systematic error stems from the uncertainty in the LEP beam energy, which was estimated to be 0.027 GeV [7]. The uncertainty coming from the knowledge of the W width was calculated in [36] and found to be negligible.

6 Conclusions

The successful increase of LEP energy up to the W pair threshold has allowed observation of the first W pairs in $\mathrm{e^+e^-}$ annihilation [37, 38]. An integrated luminosity of 11 pb^{-1} was collected in the ALEPH detector, in which all combinations of standard W decay channels have been analyzed. The signal is essentially background-free in channels where at least one of the Ws decays leptonically. The purely hadronic channel required more

sophisticated statistical analyses, but led nevertheless to a clear signal. The W pair production cross-section was extracted. The corresponding W mass is in agreement with previous direct determinations [4], and with expectations based on precise measurements [39] obtained at the Z peak and elsewhere, assuming the validity of the minimal Standard Model.

Acknowledgments

It is a pleasure to congratulate our colleagues from the CERN accelerator divisions for the successful commissioning of the superconducting accelerating system and start-up of LEP2. We are indebted to the engineers and technicians in all our institutions for their contributions to the excellent performance of ALEPH. Those of us from non-member countries thank CERN for its hospitality.

References

[1] UA1 Coll., Phys. Lett. 122B (1983) 103
[2] UA2 Coll., Phys. Lett. 122B (1983) 476
[3] UA2 Coll., Phys. Lett. 276B (1992) 354;
CDF Coll., Phys. Rev. Lett. B65 (1990) 2243 and Phys. Rev. D43 (1991) 2070;
Measurement of the W Boson Mass, FERMILAB-PUB-95/033-E.
[4] DØ Coll., presented by M. Rijssenbeek at ICHEP '96, Warsaw; M. Rijssenbeek also gave the world average.
[5] Working group on the W mass, in "Physics at LEP2", CERN 96-01 (1996) 141.
[6] CDF Coll., presented by J. Lys at ICHEP '96, Warsaw;
DØ Coll., presented by S. Protopopescu at ICHEP '96, Warsaw;
Average presented by P. Tipton.
[7] Working group on LEP energy, private communication.
[8] ALEPH Coll., Nucl. Inst. Meth. A 294 (1990) 121.
[9] ALEPH Coll., Nucl. Inst. Meth. A 360 (1995) 481.
[10] ALEPH Coll., Z. Phys. C53 (1992) 375.
[11] `BHLUMI`, version 2.01, S. Jadach et al., Phys. Lett. B253 (1991) 469; Phys. Lett. B257 (1991) 173; Phys. Lett. B260 (1991) 438; Comput. Phys. Comm. 70 (1992) 305-344.
[12] M. Skrzypek, S. Jadach, W. Placzek, Z. Was, Comp. Phys. Commun. 94 (1996) 216.
[13] E. Barberio and Z. Was, Comp. Phys. Commun. 79 (1994) 291.
[14] M. Skrzypek et al., Phys.Lett. B372 (1996) 289.
[15] V.S. Fadin, V.A. Khoze, A.D. Martin and A. Chapovsky, Durham report DTP/94/116.
[16] GRACE Manual, MINAMI-TATEYA group, KEK report 92-19 (1993).
[17] T. Sjöstrand, Comp. Phys. Commun. 82 (1994) 74.
[18] G. Gustafson, U. Pettersson and P.M. Zerwas, Phys. Lett. B209 (1988) 90;
T. Sjöstrand and V.A. Khoze, Z.Phys. C62 (1994) 281; Phys. Rev. Lett. 72 (1994) 28.
L. Lönnbald and T. Sjöstrand, Phys. Lett. B351 (1995) 293.
Working group on the W mass, in "Physics at LEP2", CERN 96-01 (1996) 190.
[19] T. Sjöstrand and V.A. Khoze, Z. Phys. C 62 (1994) 281.
[20] Working Group on QCD Event Generators, in "Physics at LEP2", CERN 96-01 (1996), vol. 2, 103.
[21] F.A. Berends, R. Pittau and R. Kleiss, Comp. Phys. Commun. 85 (1995) 437.

[22] F.A. Berends, G. Burgers and W.L. Van Neerven Phys. Lett. B185 (1987) 395; Nucl. Phys. B297 (1988) 429, E: Nucl. Phys. B304 (1988) 921.
[23] ALEPH Coll., Phys. Lett. 313B (1993) 509.
[24] S. Jadach, B.F.L. Ward, Z. Was, Comp. Phys. Commun. 79 (1994) 503.
[25] H. Anlauf et al, Comp. Phys. Commun. 79 (1994) 466.
[26] J.M. Hilgart, R. Kleiss and F. Le Diberder, Comp. Phys. Commun. 75 (1993) 191.
[27] W. Bartel et al, JADE Coll., Z. Phys. C 33 (1986) 23; S. Bethke et al, JADE Coll., Phys. Lett. B213 (1988) 235.
[28] Yu.L. Dokshitzer, J. Phys. G17 (1991) 1441.
[29] S. German, E. Bienenstock, R. Doursat, Neural Computation 4 (1992) 1.
[30] Ll. Garrido and V. Gaitan, Int. J. Neural Sys. 2 (1991) 221;
S. Gomez and Ll. Garrido, Int. J. Neural Sys. 7, N. 1 (1996) 19 ;
D.W. Ruck et al., IEEE Transactions on Neural Networks, 1 (1990) 296;
E.A. Wan, IEEE Transactions on Neural Networks, 1 (1990) 303.
[31] F. Le Diberder, Mark II/SLC Note #245 (1989).
[32] R. Barlow, J. Comp. Phys 72 (1986) 202.
[33] G. Marchesini and B.R. Webber, Nucl. Phys. B310 (1988) 461;
I. Knowles, Nucl. Phys. B310 (1988) 571;
G. Marchesini et al., Comp. Phys. Comm. 67 (1992) 465.
[34] L. Lyons et al., NIM A270 (1988) 110.
[35] D. Bardin, A. Leike, T. Riemann, Phys. Lett. B344 (1995) 383
[36] W.J. Stirling, Nucl. Phys. B456 (1995) 3.
[37] OPAL Coll., Phys. Lett. B389 (1996) 416.
[38] DELPHI Coll., CERN-PPE/97-09 (1997);
L3 Coll., CERN-PPE/97-14 (1997).
[39] The LEP Collaborations and the LEP Electroweak Working Group, CERN-PPE/96-183 (1996).